A Realistic Simulation Model for Uranium Series Geochronological Dating

Cheng Yeng Hung*

Abstract

This paper presents a simulation model for uranium series geochronological dating employed in adjusting the age of the earth claimed by evolutionary scientists. The model assumes that decay half-lives have been constant throughout earth history, but introduces detailed equations to simulate diffusion and migration of radionuclide through a porous medium. Theoretically, a radiometric-dating model should be developed based on the solute transport theory, which involves tedious numerical computation. However, the traditional model imposes two crude assumptions to simplify the computational processes, even though it is known that inevitable errors may result. They are: (1) mineral deposits are confined in a closed system and no radionuclide migration can take place, and (2) the decay chain is in its "ultimate" equilibrium at the time of dating. On the other hand, the proposed simulation model calculates the age of minerals based on the solute transport theory. As such, the errors inherited in the traditional model can be minimized or avoided. The results of model verification indicate that there are excellent agreements between the simulation results and the analytical solutions for two cases: radioactive decay and diffusion. Comparison of the results indicates that the closed system assumption results in overestimation of the age of mineral when the age exceeds the "critical year." A comparison of an existing study for a rhyolite from the Cobb Mountain, California and results from the simulation model also show the same trend.

Introduction

The dispute about the age of earth between evolutionary scientists and biblical creationary scientists has continued for centuries. Evolutionists now claim an age of 4.5 billion years for the age of the earth, whereas biblical creationists claim an age of no more than 8,000 years. In spite of recent progress, I do not see that a satisfactory solution has been proposed to reconcile this dispute. Since the radiometric dating method is the most important means of determining the age of the earth by scientists, it is important to evaluate the accuracy of this dating method.

* Cheng Yeng Hung, 6178 Hardy Drive, McLean, VA 22101,
   Phone: (703) 893-6833, E-mail: chengandme@msn.com
   (Retired from Office of Radiation and Indoor Air,
   U.S. Environmental Protection Agency, Washington, D.C.)

A preliminary investigation revealed that a radiometric-dating model should be developed based on solute transport theory, which involves tedious numerical process. The solute transport theory depicts the relationships between the rate of transport of embed radioactive nuclei (radionuclides) in a porous medium and the characteristics of the medium and radionuclides. The medium is assumed to have a finite ability to conduct the solute transport in a fluid solvent via fluid flow, which can diffuse and migrate. This is modeled using *solute transport system equations.* The traditional model imposed two crude assumptions to simplify the computational processes, knowing inevitable errors may result. They are (1) the radionuclides in the mineral deposit are confined in a closed compartment and no radionuclide migration can take place (closed-system assumption), and (2) the radioactive decay series is in its ultimate equilibrium stage at the time

of dating (ultimate-equilibrium assumption) (e.g., Nier et al., 1941; Wetherill, 1956; Tera and Wasserburg, 1972; Compston et al., 1985; Durrance, 1986, p. 287; Getty and DePaolo, 1995; Neymark et al., 2000; Pike et al., 2002; Tera, 2003; Mundil et al., 2004; Chang et al., 2006; van Calsteren and Thomas, 2006).

An ultimate-equilibrium stage is defined as a stage when the ingrowth of the stable radionuclide in a decay chain reaches to the same decay rate of its parent nuclide. In reality, a ^{238}U radionuclide decays into ^{234}U, ^{230}Th, ^{226}Ra, and finally to ^{206}Pb (taking into account only the long half-life radionuclides). In the beginning, the rate of ingrowth of ^{206}Pb will be much smaller than the decay rate of ^{238}U. However, the discrepancies between these two rates become smaller and smaller with the increase in the duration of decay, and eventually reaches zero or ultimate equilibrium.

Because the ratio of the stable daughter nuclide to the remaining parent nuclide is used to measure the age of minerals, ignoring the migration loss of both parent and daughter nuclides and the distorted ultimate-equilibrium assumption could potentially create significant error in dating. This potential error has been pointed out by numerous investigators (e.g., Szabo and Rosholt, 1969; Hille, 1979; Durrance, 1986, p. 306; Pike et al., 2002; Tera, 2003; van Calsteren and Thomas, 2006). Nevertheless, the dating methods using these crude assumptions continue to dominate the field of geochronology.

To improve the accuracy of radiometric dating, a simulation model that considers the migration of radionuclide and transient radionuclide decay is needed to simulate the dynamics of the radiometric-dating system. With the advanced computer modeling techniques available today, employing a dynamic simulation model for radiometric dating is now realistically possible.

This paper presents the performance of the simulation model employed in adjusting the age of earth claimed by scientists. The model is designed to transport the parent and daughter nuclides from the crystallized mineral deposit to the ambient crystalline rock in a three dimensional (3-D) system. The transport processes include convective and dispersive transport and molecular diffusion, as well as transient radioactive decay processes. A ^{238}U-^{206}Pb series method is selected because this method is one of the most important methods used in determining the age of the earth. Model verification on the decay and diffusion processes is also conducted for checking the credibility of the model.

Theoretical Background of Dating Model

Generic Mass-Transport System Equation

The basic equations governing a mass-transport system were well established by previous investigators (e.g., Duguid and Reeves, 1976; Pinder and Gray, 1977; Huyakorn et al., 1986;

McDonald and Harbaugh, 1988; Anderson and Woessner, 1992; Hydrogeologic, Inc., 1995; Leake and Lilly, 1997; Yeh et al., 2002; and Hung, 1986, 2000, and 2004). Although the basic form of the system equations derived by each investigator vary slightly, the generic form can be summarized as follows.

Flow System Equation: The generic flow system equations for a steady flow in a heterogeneous, anisotropic, and variably saturated porous medium can be summarized in a Cartesian coordinate system as:

$$v_i = -K_i k_{rw} \frac{\partial h}{\partial x_i} \tag{1}$$

(for i = 1 to 3)

for the equation of motion and

$$\sum_{i=1}^{3} \frac{\partial}{\partial x_i}\left(K_i k_{rw} \frac{\partial h}{\partial x_i} \right) = 0 \tag{2}$$

for the continuity equation (Bear, 1979). In the above equations, v_i are the components of Darcy velocity, K_i are the components of saturated hydraulic conductivity, k_{rw} is the relative conductivity, h is the hydraulic head, and x_i are the spatial coordinates.

Equation (1) expresses the postulated assumption that fluid will migrate away from regions of high hydraulic pressure (head) h and toward regions of low hydraulic pressure h. Equation (2) expresses the continuity condition, which basically states that fluid is not created or destroyed but may migrate across boundaries.

Solute Transport System Equation: The generic solute transport system equation for the kth radionuclide in a ℓ member decay chain can be summarized as (Bear, 1979):

$$\frac{\partial}{\partial x_i}\left(D_{ij} \frac{\partial c_k}{\partial x_j} \right) - v_i \frac{\partial c_k}{\partial x_i} = \phi S_w R_k \frac{\partial c_k}{\partial t}$$
$$+ \phi S_w R_k \left(\lambda_k c_k - \frac{A_k R_{k-1}}{A_{k-1} R_k} \lambda_{k-1} c_{k-1} \right) \tag{3}$$

(for i = 1 to 3, j = 1 to 3, and k = 1 to ℓ when k-1 >0)

where D_{ij} is the component of apparent hydrodynamic dispersion tensor, c_k is the concentration of the kth daughter nuclide in the ℓ member decay chain desorbed in the water; v_i is the Darcy velocity; Φ is the effective porosity, S_w is the degree of water saturation, R is the retardation factor, λ is the radionuclide decay constant, A is the atomic weight, and subscripts

k, i and j represent the order of daughter nuclide in the decay series and spatial coordinates x, y and z. Here the Einstein summation convention is followed, that the repeated indices i and j are summed over from 1 to 3.

Traditional Model

The processes of solving the above dynamic equations are extremely complex, involving long and intricate mathematical analyses. To avoid these complex processes, the traditional model simplifies them by imposing two crude assumptions: closed-system and ultimate-equilibrium assumptions.

The first assumption eliminates the necessity of the flow equations—Equations (1) and (2)—and the transport terms in the solute transport equation. As a result, the governing system equations are simplified into the form:

$$\frac{\partial c_k}{\partial t} + \left(\lambda_k c_k - \frac{A_k}{A_{k-1}} \lambda_{k-1} c_{k-1} \right) = 0 \qquad (4)$$

(for k = 1 to ℓ when k-1 >0)

Despite the fact that an analytical solution can be obtained from Equation (4), previous investigators simplified the solution further by imposing the second assumption, which assumed the rate of ingrowth of ^{206}Pb is in equilibrium with the rate of ^{238}U decay loss. That is, it assumes that ^{238}U decays into ^{206}Pb directly. ^{206}Pb is stable and thus has zero decay constant; hence, assuming that the first term in Equation (4) represents the ingrowth of ^{206}Pb for k = 2 (final member of the decay chain), then this rate should be equal to the decay rate of ^{238}U (k-1=1). The solution of this simplified differential equation is shown by Durrance (1986) or Getty and DePaolo (1995) as:

$$^{206}Pb(t) = {}^{206}Pb(0) + {}^{238}U(t) \cdot [Exp(\lambda_{238}t) - 1]$$

$$(5)$$

In Equation (5), λ_{238} represents the decay constant for ^{238}U, t represents the time, and ^{206}Pb and ^{238}U represent the number of atoms for ^{206}Pb and ^{238}U, respectively.

When this assumption is imposed, the age of the mineral can then be calculated from Equation (5) as:

$$t = \frac{1}{\lambda_{238}} \log_e \left[\frac{{}^{206}Pb(t)}{{}^{238}U(t)} - \frac{{}^{206}Pb(0)}{{}^{238}U(t)} + 1 \right] \qquad (6)$$

That is, the age of the mineral can be calculated from Equation 6 once the ^{206}Pb/^{238}U ratio of the mineral is measured and its ^{206}Pb(0)/^{238}U(t) ratio is properly estimated. Equation (6) is the basic equation of the traditional model.

Proposed Dynamic Simulation Model

The proposed simulation model is designed to simulate the transport of radionuclides based on the basic equations described above. Existing models, such as the MODFLOW (MODular FLOW) –SURFACT (integrated with a new efficient Scheme to treat Unconfined, non-ponding Recharge, and Fracture well flow modules for the Analysis of Contaminated Transport) model (Hydrogeologic, Inc., 2001) or GMS (Groundwater Modeling System) model (U.S. Army Waterways Experiment Station, 2002), were designed for comprehensive environmental engineering applications. Therefore, direct application of these models may suffer from difficulties of (1) modeling the intended conceptual model accurately, (2) prolonged duration of analysis, and (3) extracting the required specific output values. Therefore, a new model is needed for exclusive radiometric-dating application.

Conceptual Model

The conceptual model assumes a mineral is deposited at the center of a homogeneous anisotropic host formation in the earth crust and is exposed to the natural geohydrological envi-
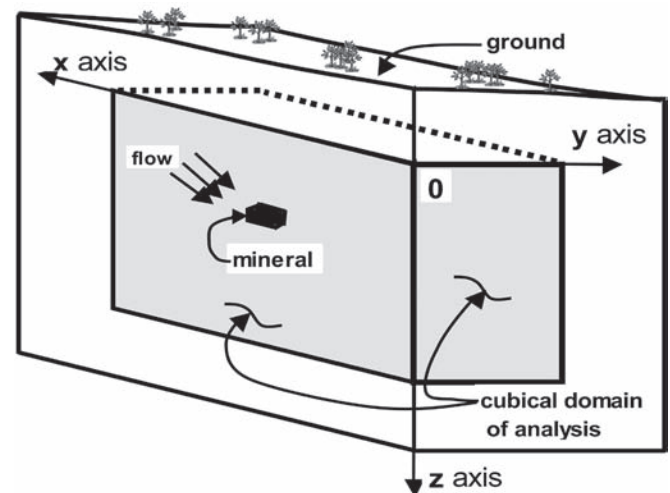

Figure 1. Schematic of the conceptual model for the simulation model. It shows the geohydrological environment after the mineral is deposited in the earth crust as an open system.

ronment, including convective and dispersive transports from the ambient groundwater flow. Figure 1 shows the schematic of this conceptual model.

Flow-System Equation

The mineral and its ambient host rock selected for radiometric dating are normally crystallized and nonporous in texture and underlain below the ground surface. Therefore, the transport media, including mineral and host rock, would have very low percentage of gravity water porosity (Hillel, 1980; Hung, 1983 and 2005). It follows that the transport media is constantly saturated with pellicular water (*pellicular water* is the moisture content in the porous media that cannot be lost by gravity drainage process but by natural drought process) even under unsaturated flow conditions. Thus, the hydraulic conductivity of the mineral and the host rock will always exhibit their near-saturated hydraulic conductivity, respectively (Hillel, 1980; Hung, 1983 and 2005).

Therefore, the basic flow-system equations to be used in the simulation model, Equations (1) and (2), can be simplified and expanded as:

$$
\begin{aligned}
v_x &= -K_x \frac{\partial h}{\partial x} \\
v_y &= -K_y \frac{\partial h}{\partial y} \\
v_z &= -K_z \frac{\partial h}{\partial z}
\end{aligned}
\tag{7}
$$

and

$$
\frac{\partial}{\partial x}\left(K_x \frac{\partial h}{\partial x}\right) + \frac{\partial}{\partial y}\left(K_y \frac{\partial h}{\partial y}\right) + \frac{\partial}{\partial z}\left(K_z \frac{\partial h}{\partial z}\right) = 0
\tag{8}
$$

The space-dependent components of the velocity vector can therefore be solved independently. The results of the flow-system analysis can then be applied to the solute-transport-system analysis.

Solute-Transport-System Equation

As discussed above, the relative hydraulic conductivity and the degree of water saturation can be approximated as unity. It follows that Equation (3) can be expanded as:

$$
\frac{\partial}{\partial x}\left(D_{xx}\frac{\partial c_k}{\partial x}\right) + \frac{\partial}{\partial x}\left(D_{xy}\frac{\partial c_k}{\partial y}\right) + \frac{\partial}{\partial x}\left(D_{xz}\frac{\partial c_k}{\partial z}\right)
$$

$$
-v_x\frac{\partial c_k}{\partial x} + \frac{\partial}{\partial y}\left(D_{yx}\frac{\partial c_k}{\partial x}\right) + \frac{\partial}{\partial y}\left(D_{yy}\frac{\partial c_k}{\partial y}\right)
$$

$$
+\frac{\partial}{\partial y}\left(D_{yz}\frac{\partial c_k}{\partial z}\right) - v_y\frac{\partial c_k}{\partial y} + \frac{\partial}{\partial z}\left(D_{zx}\frac{\partial c_k}{\partial x}\right)
$$

$$
+\frac{\partial}{\partial z}\left(D_{zy}\frac{\partial c_k}{\partial y}\right) + \frac{\partial}{\partial z}\left(D_{zz}\frac{\partial c_k}{\partial z}\right) - v_z\frac{\partial c_k}{\partial z}
$$

$$
= \phi S_w R_k \frac{\partial c_k}{\partial t} + \phi S_w R_k \left(\lambda_k c_k - \frac{A_k R_{k-1}}{A_{k-1} R_k}\lambda_{k-1} c_{k-1}\right)
$$

$$
\tag{9}
$$

In Equation (9), c_k is the concentration of the kth decay member radionuclide. The components of the apparent hydrodynamic dispersion tensor, D_{xx}, D_{xy}, D_{xz}, D_{yx}, D_{yy}, D_{yz}, D_{zx}, D_{zy}, and D_{zz} are space dependent and given by Scheidegger (1961), and Burnett and Frind (1987), for stratified porous media as:

$$
D_{xx} = \alpha_{Lh}\frac{v_x^2}{|v|} + \alpha_{Th}\frac{v_y^2}{|v|} + \alpha_{Tv}\frac{v_z^2}{|v|} + \beta D_0
$$

$$
D_{yy} = \alpha_{Th}\frac{v_x^2}{|v|} + \alpha_{Lh}\frac{v_y^2}{|v|} + \alpha_{Tv}\frac{v_z^2}{|v|} + \beta D_0
$$

$$
D_{zz} = \alpha_{Tv}\frac{v_x^2}{|v|} + \alpha_{Tv}\frac{v_y^2}{|v|} + \alpha_{Lv}\frac{v_z^2}{|v|} + \beta D_0
$$

$$
D_{xy} = D_{yx} = (\alpha_{Lh} - \alpha_{Th})\frac{v_x v_y}{|v|}
$$

$$
D_{xz} = D_{zx} = \left(\frac{\alpha_{Lh} + \alpha_{Lv}}{2} - \alpha_{Tv}\right)\frac{v_x v_z}{|v|}
$$

$$
D_{yz} = D_{zy} = \left(\frac{\alpha_{Lh} + \alpha_{Lv}}{2} - \alpha_{Tv}\right)\frac{v_y v_z}{|v|}
$$

$$
\tag{10}
$$

where α is the dispersivity, β is the tortuosity, D_0 is the free-water molecular diffusion coefficient, and the subscripts Lh, Th, Lv, and Tv are indices for horizontal longitudinal, horizontal transverse, vertical longitudinal, and vertical transverse direction respectively. *Tortuosity* refers to the ratio of the diffusion

coefficient in the porous medium to the diffusion coefficient D_0 in free space. Usually it is smaller than unity in the medium since the solid particles in the medium impede the flow, or cause a *tortuous path* for the diffusion.

Model Development

Basic Equations

As shown in Equation (9), the time derivative of the radionuclide concentration is a linear sum of the transport effect, and the decay/ingrowth effect. To simplify the modeling processes, these two effects are separated in the model implementation. After the separation, the basic equations are expressed in

$$
\begin{aligned}
\frac{\partial c_k}{\partial t} = \frac{1}{\phi S_w R_k} & \left\{ \frac{\partial}{\partial x}\left(D_{xx}\frac{\partial c_k}{\partial x}\right) + \frac{\partial}{\partial x}\left(D_{xy}\frac{\partial c_k}{\partial y}\right) \right. \\
& + \frac{\partial}{\partial x}\left(D_{xz}\frac{\partial c_k}{\partial z}\right) - v_x\frac{\partial c_k}{\partial x} + \frac{\partial}{\partial y}\left(D_{yx}\frac{\partial c_k}{\partial x}\right) \\
& + \frac{\partial}{\partial y}\left(D_{yy}\frac{\partial c_k}{\partial y}\right) + \frac{\partial}{\partial y}\left(D_{yz}\frac{\partial c_k}{\partial z}\right) - v_y\frac{\partial c_k}{\partial y} \\
& + \frac{\partial}{\partial z}\left(D_{zx}\frac{\partial c_k}{\partial x}\right) + \frac{\partial}{\partial z}\left(D_{zy}\frac{\partial c_k}{\partial y}\right) \\
& \left. + \frac{\partial}{\partial z}\left(D_{zz}\frac{\partial c_k}{\partial z}\right) - v_z\frac{\partial c_k}{\partial z}\right\}
\end{aligned}
$$

$$(11)$$

$$
\frac{\partial c_k}{\partial t} = \left(\frac{A_k R_{k-1}}{A_{k-1}R_k}\lambda_{k-1}c_{k-1} - \lambda_k c_k \right) \tag{12}
$$

respectively, representing the transport component and decay/ingrowth component.

A standard central difference scheme is selected for the numerical analysis of the transport component. The computer code for this component is implemented in the main program. More details of the formulation of the model are given in Appendix A.

Model Verification

The computer encoding and model verification can be tested for some limiting cases. Two independent processes are selected: radioactive decay and hydrodynamic transport. The results of verification are detailed as follows.

Radioactive Decay Process

During the course of verifying the radioactive decay process, the portion of simulation for the hydrodynamic transportation is bypassed, so that the source of [238]U and its progenies are assumed to remain in the designated compartment as a closed system. For the purpose of model verification, it is assumed that one mole of [238]U is placed at the center of the simulation field. We are not necessarily assuming that this is a realistic assumption; we are just using it to test the computer code and the model on which it is based. The simulation is conducted for 10,000,000 years in which the masses of parent and its progenies are integrated. The results of simulation for all five radionuclides in the decay chain, [238]U, [234]U, [230]Th, [226]Ra, and [206]Pb, are printed out for the target year of 100, 1,000, 10,000, 100,000, 1,000,000, and 10,000,000.

In parallel to the simulation, the decay/ingrowth products from the same one mole of [238]U are also calculated utilizing the Bateman equation detailed in Appendix B.

The results of the analysis are plotted together with the results of simulation and presented in Figure 2. The results obtained from the analytical solution and the simulation model agree with each other very well, confirming that the mathematical formulas and the computer codes developed for the decay portion are valid.

Transport Process

Because the simulation model is designed for a very low hydraulic conductivity condition, the entire radionuclide transport process is predominated by the dispersion/diffusion process. Therefore, for the purposes of model verification, the analytical solution representing point source diffusion in an infinite space is selected. As derived by Crank (1975), the analytical solution for a point source at the center of an infinite space takes the form

$$
C = \frac{M}{8(\pi D t)^{3/2}} Exp(-\frac{r^2}{4Dt}) \tag{13}
$$

where C is the concentration of diffusing substance, M is the source strength, D is the diffusion coefficient, r is the distance from the source, and t is the time elapsed.

By assuming the source strength is 100 grams and the diffusion coefficient is 0.01 cm²/yr, the distribution of concentrations around the source point is calculated from Equation (13) for one, two, three, and four years after diffusion has commenced. The results of these calculations are presented in Figure 3.

To verify the simulation model, comparable source strength of 100 grams is placed at the center of the digitized three-dimensional space. The components of the equivalent
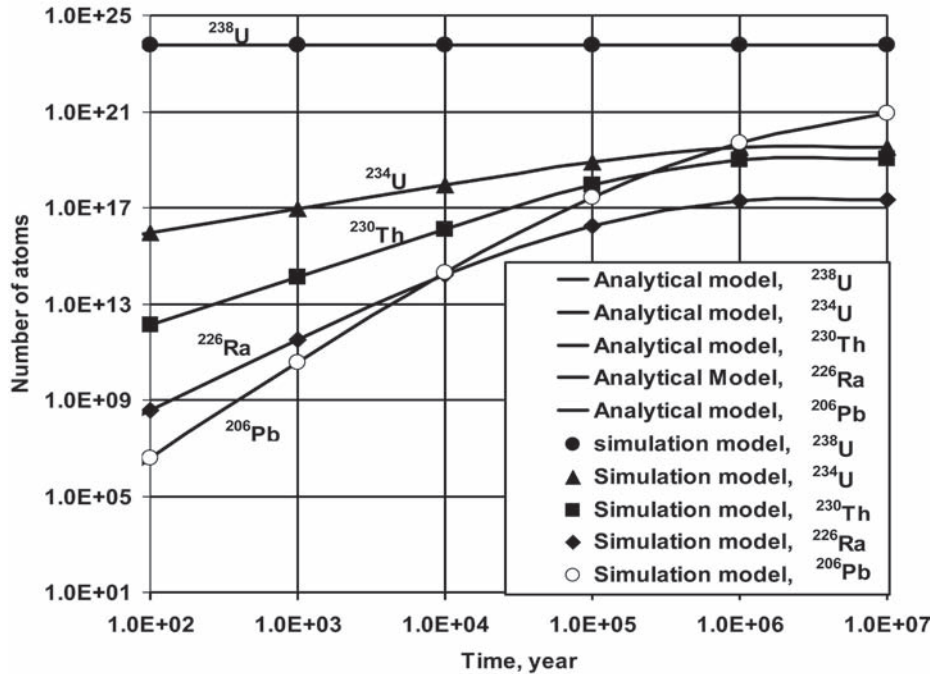
Figure 2. Comparison of the results of radionuclide decay/ingrowth obtained from analytical and dynamic simulation models. The initial ^{238}U strength is assumed to be 1 mole for both calculations. The close match of these two solutions validates the simulation model.
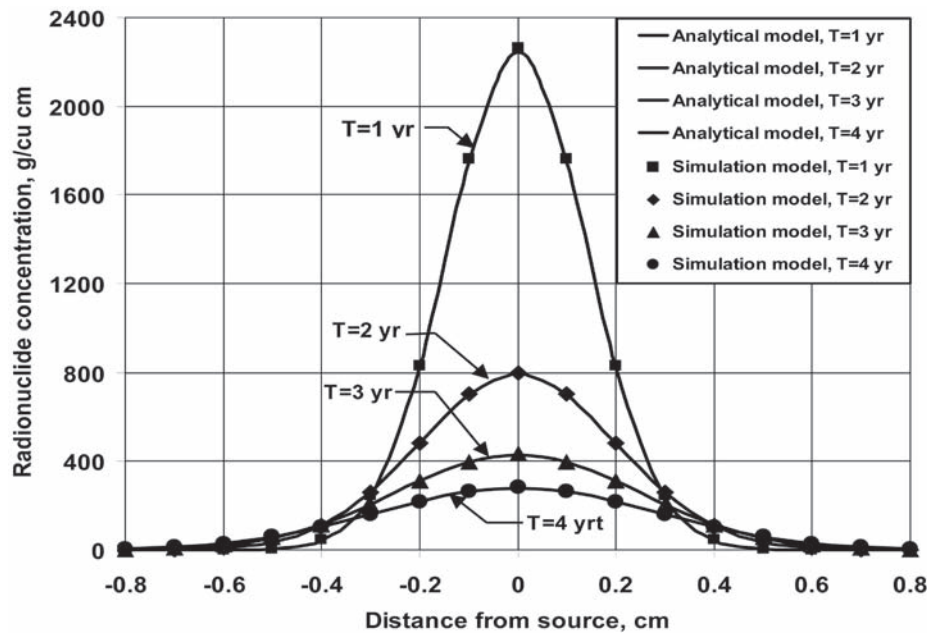

Figure 3. Comparison of the results of radionuclide concentrations obtained from analytical and dynamic simulation models. The source strength and the diffusion coefficient are assumed to be 100 grams and 0.01 cm²/yr, respectively. The close match in the concentration distribution between the results of simulation and analytical solutions validates the simulation model.

diffusion coefficients in the x, y, and z directions are maintained at 0.01 cm²/yr, and their space increments are maintained at 0.05 cm. The simulation suppresses the radioactive decay and convective transport effects by bypassing the radioactive decay and convective transport processes. The results of concentration simulation are also plotted for one, two, three, and four years after the commencement of diffusion and for the spaces at 0.0, 0.1, 0.2, 0.3, 0.4, 0.5, 0.6, 0.7 and 0.8 cm from the source, respectively, on Figure 3. Figure 3 shows that the concentrations obtained from the simulation model and the analytical model agree each other very well. This also implies that the model equation and numerical algorithm used in the model for dispersion process are accurate and valid.

Because the convective flow portion of the model is a simple addition of numerical scheme to the dispersion process, the transport portion of the simulation is also considered to be accurate. From the results above, one can claim that this simulation model is accurate and valid.

Comparison of Simulation and Traditional Models

Scenario of Analyses

For the simulation model, it is assumed that one unit mass of pure ^{238}U is deposited at the center of the domain of analysis. During the process of simulation, the model calculates the variation of the mass of each radionuclide in the decay chain and the ^{206}Pb/^{238}U ratio with time. As to the traditional model, the time variation of the ^{206}Pb/^{238}U ratios is calculated through Equation (6) by assuming there is no initial mass of ^{206}Pb, which matches with simulation model analysis.

Table I. Collected porosity and density of rocks and mineral from the work of Ho et al. (1989).

Transport media	Porosity, unit-less	Density, g/cm³
granite	0.03*	2.67*
basalt	0.03	2.67
mineral	0.01	2.65

Note: * denotes the value used for the ambient host rock.

Input Data Collection

The key to generate accurate results from a dynamic simulation is to use the most accurate input parameters. Fortunately, existing studies provide enough valid data for this generic site study. To execute the simulation model, the following input parameters are needed: porosity, density, hydraulic conductivity, dispersivity, free-water molecular diffusion coefficient, distribution coefficient, and radionuclide decay-constant. The collected decay constant for ^{238}U is also used for the traditional model.

Porosity and Density: Extensive porosity and density data for various igneous and sedimentary rocks have been compiled based on the site-specific field data collected by various investigators (Ho et al., 1989). More than 60 sites for sandstone and nearly 20 sites for granite have been compiled. Nevertheless, for the purposes of this study, conservative values are selected for the model input (Table I.)

Hydraulic Conductivity and Dispersivity: The hydraulic conductivity and dispersivity data have been studied and collected by Ho et al. (1989). Together, 11 sites of granite, 6 sites of basalt, and 65 sites of sandstone hydraulic conductivity data, along with 8 sites of basalt and sedimentary rock for dispersivity were collected. Based on these field and laboratory

data, the conservative values of the hydraulic conductivity and dispersivity are determined for use in this simulation study (Table II.)

Free-Water Molecular Diffusion Coefficient: The free-water molecular diffusion coefficients for various chemical species in water have been collected by Bird et al. (1960) and Thibodeaux (1979). The collected data varies with chemical species and range from 0.2×10^{-5} to 2.0×10^{-5} cm²/sec. Considering only low concentration chemical species and low temperature applications, the most conservative value (the lowest diffusion coefficient), 0.2×10^{-5} cm²/sec (63.1 cm²/yr), is selected for chemical species considered in this study

Distribution Coefficient: Extensive distribution coefficient studies have been conducted for a wide range of radioactive chemical species based on actual laboratory and in-situ measurements (USEPA, 1999a). Although the distribution coefficients may vary widely with the chemical environment, the site-specific data collected in conjunction with the risk assessment of radioactive waste disposal sites (USDOE, 1992; SNL, 1996; USEPA, 1999b) are most suitable for this study. This is because the collected data were all measured under natural groundwater flow environment, which matches with the environment expected in this study.

Because of the non-site-specific nature of this study, the most conservative coefficients (highest values being collected for the above three sites) are selected for the host rock and an additional 20 % is added for the mineral deposit. The selected distribution coefficients for the host rock and mineral deposit are summarized and shown in Table III.

Radioactive Decay Constant: The radioactive decay constants for the known radionuclides are thoroughly investigated and compiled in various radiological handbooks. Normally, the characteristics of radionuclide decay constants are compiled in half-life, from which the radioactive decay constant can be calculated. The half-life of the radionuclides are collected to be 4.468E+9, 2.445E+5, 7.7E+4, 1.6E+3 years for

Table II. Collected hydraulic conductivities and dispersivities from the work of Ho et al. (1989).

Transport media	Hydraulic conductivity, cm/sec		Dispersivity, m		
	Horizontal	Vertical	Longitudinal	Lateral	Vertical
granite	4.0E-9*	2.0E-9*	0.1*	0.05*	0.05*
basalt	4.0E-9	2.0E-9	0.1	0.05	0.05
mineral	4.0E-10	2.0E-9	0.1	0.05	0.05

Note: * denotes the value used for the ambient host rock.

Table III. Collected distribution coefficients (k_d). They are characterized by the chemical species instead of radio-nuclide and are collected from the work of government agencies and national laboratories (USDOE, 1992; SNL, 1996; USEPA, 1999b).

Nuclide	Host rock (ml/g)	Mineral deposit (ml/g)
uranium (U)	50	60
thorium (Th)	3200	3840
radium (Ra)	700	840
lead (Pb)	270	324

^{238}U, ^{234}U, ^{230}Th, ^{226}Ra and stable for ^{206}Pb, respectively (US Department of Health, Education, and Welfare, 1970; Shleien et al., 1998).

Results and Discussion

The results of ^{206}Pb/^{238}U ratio analyses for the traditional model and simulation model are plotted and presented in Figure 4. A comparison of the results indicates that both the simulation model and the traditional model exhibit the same ^{206}Pb/^{238}U ratio at near 42,000 years. For the purpose of this study, this year is defined as the "critical year or age." Figure 4 also indicates that the traditional model underestimates the age of the mineral before the age reaching the critical year. Conversely, it overestimates the age after the age exceeds the critical year.

One should notice that the variation of the discrepancies between the traditional model and simulation model are caused by the combined effects of ultimate-equilibrium assumption and closed-system assumption. The underestimate of the age by the traditional model, when the age is younger than the critical age, is due to the predominated effect from the ultimate-equilibrium assumption. Conversely, the overestimate of the age, when the age of the mineral exceeds the critical age, is due to the predominated effect from closed-system assumption. Thus, the intersection of the two curves at the

critical year signifies the time when the two effects compensate each other.

A sub-scenario of unsaturated groundwater-flow conditions is also analyzed and added to Figure 4 to see the effects of unsaturated groundwater-flow conditions. The same figure indicates that there are only minor effects from unsaturated conditions. This is because there are very limited gravity water voids in the host rock and mineral, which are always saturated with pellicular water even under unsaturated condition (Hillel, 1980; Hung, 1983 and 2005).

Comparison with Existing Study

A relatively recent study has been reported by Getty and De-Paolo (1995) for dating a rhyolite from the Cobb Mountain volcanic field located 100 km north of San Francisco, California. The study used the measured ^{238}U/^{207}Pb ratio and ^{206}Pb/^{207}Pb ratio data for albite, sanidine, matrix (surrounding fill rock), and ilmenite to plot the variation line on the ^{206}Pb/^{207}Pb ratio vs. ^{238}U/^{207}Pb ratio plan. Using the measured slope of the ^{206}Pb/^{207}Pb vs. ^{238}U/^{207}Pb variation line of 0.00016 (equivalent to ^{206}Pb/^{238}U ratio), the age of the rhyolite was calculated to be 1.03 million years ago (Ma). Applying the same ^{206}Pb/^{238}U ratio of 0.00016 to the traditional model and simulation model resulted in 1.05 Ma for the traditional model and 0.0735Ma for the simulation model. These results together with that
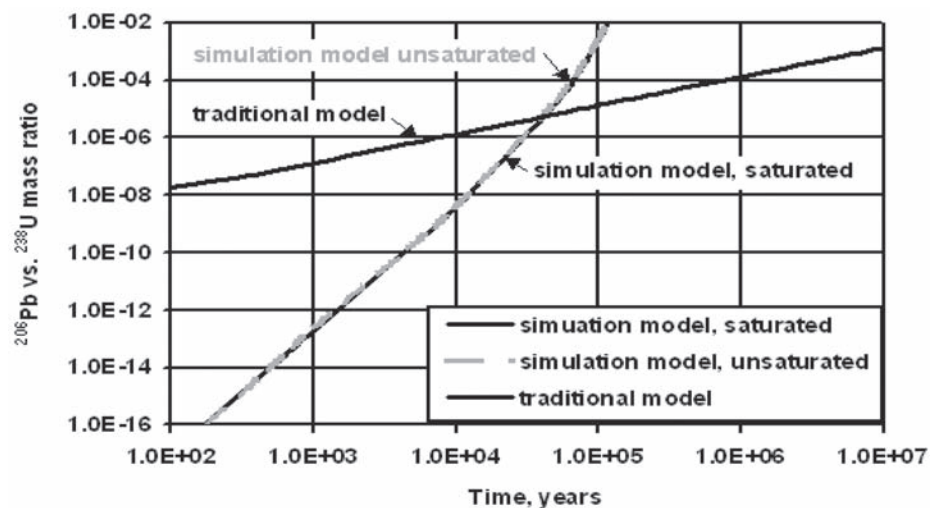

Figure 4. Comparison of the results of ^{206}Pb/ ^{238}U ratio analyses for the dynamic simulation model and the traditional model. This figure shows that the closed system model will underestimate the age when the age is less than the critical year. Conversely, it will overestimate the age when the age of mineral exceeds the critical year.
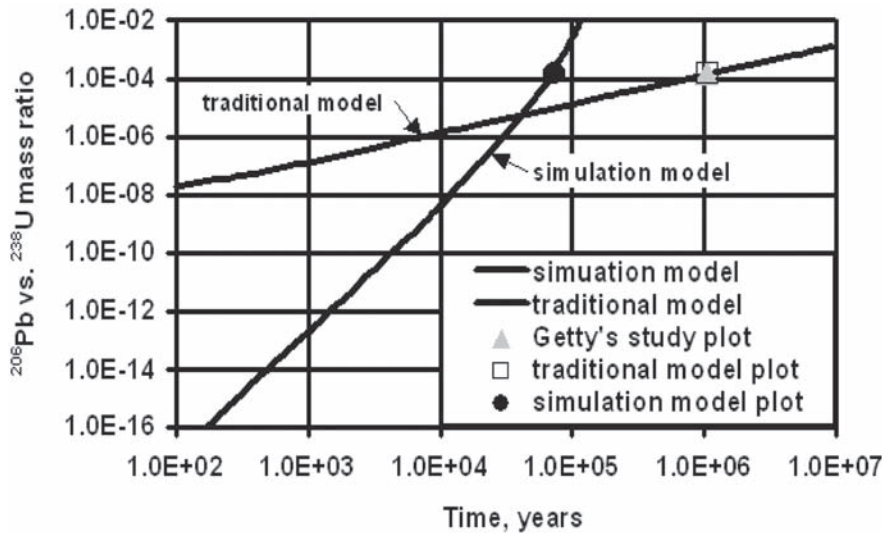
Figure 5. Comparison of the results of existing dating study for a rhyolite from the Cobb Mountain volcanic field using Getty and DePaolo's approach, dynamic simulation model, and traditional model. The results obtained from the traditional model are practically identical to the result obtained from Getty and Depaolo's approach. However, the dating result obtained from the dynamic simulation model is much smaller than that reported in Getty and DePaolo's study. The relative error is as high as 92.9%.

obtained from Getty and DePaolo's study are added to Figure 4 and presented in Figure 5. The results obtained from the traditional model are practically identical to that reported in Getty and DePaolo's study. However, there are significant differences between the ages obtained from simulation model and that from Getty and Depaolo's study. These differences are caused by the fact that the simulation model considers the transport of radionuclides out of the mineral deposit, whereas Getty and Depaolo study did not. The relative error is calculated to be on the order of 92.9%.

Conclusions

A 3-D dynamic simulation model that takes into consideration the dynamic transport of radionuclides associated with decay/ingrowth processes has been developed. This model is verified for both the decay/ingrowth and for the transport components. The results of model verification indicate that there are close agreements between the results of simulation and analytical solutions, implying that the model is valid and accurate.

In order to demonstrate the performance of the model, the time variation of $^{206}Pb/^{238}U$ ratios are analyzed for both using the dynamic simulation model and the traditional model. The results of analyses indicate that the traditional model will underestimate the age of mineral when the ages are below the

critical year and, conversely, will overestimate the age when the age exceeds the critical year. These overestimates or underestimates are caused by the crude assumptions (closed-system assumption and ultimate-equilibrium assumption) being imposed on the traditional model to simplify the processes of model analysis. Since the range of age interest is normally greater than the critical year, one may claim that the traditional model will, in general, overestimate the age of mineral.

The result of comparison with the existing study conducted for the Alder Creek rhyolite by Getty and DePaolo also experienced the same result, 0.0735 Ma from simulation model versus 1.03 Ma from Getty and DePaolo's study. This is because Getty and DePaolo's study also had imposed the closed-system and ultimate-equilibrium assumptions.

The conclusions of the study thus include that for many samples traditionally given millions of years of age by evolutionists, the age is reduced when the more realistic diffusion and flow models are used. However, they are not necessarily reduced by the amounts that a biblical time frame would require.

Appendix A. The Model Used for Numerical Analysis

Radionuclide Decay Subroutine

A quasi-analytical scheme is employed for the numerical analysis of the decay/ingrowth component to improve the accuracy of simulation. This scheme employs the well-known analytical solution derived by Bateman (Bateman, 1910; and Evans, 1967, p. 490) to calculate the increment of radionuclides concentration. Furthermore, to improve the accuracy of numerical analysis, the calculation for each time step is subdivided into two parts, with each part accounting for the effects accrued in one-half of the time step. With a maximum of five decay-chain members and with a time increment of $0.5\Delta t$, the concentration of each radionuclide in the decay chain takes the form:

$$c_1(t - 0.5\Delta t, x, y, z) = c_1(t - \Delta t, x, y, z)\,Exp(-\lambda_1\,0.5\Delta t)$$

$$c_2(t - 0.5\Delta t, x, y, z) = \lambda_1 c_1(t - \Delta t, x, y, z)\left(\frac{A_2 R_1}{A_1 R_2}\right)\left[\frac{Exp(-\lambda_1\,0.5\Delta t)}{(\lambda_2 - \lambda_1)}\right.$$

$$\left. + \frac{Exp(-\lambda_2\,0.5\Delta t)}{(\lambda_1 - \lambda_2)}\right] + c_2(t - \Delta t, x, y, z)\,Exp(-\lambda_2\,0.5\Delta t)$$

$$c_3(t - 0.5\Delta t, x, y, z) = \lambda_1 \lambda_2 c_1(t - \Delta t, x, y, z)\left(\frac{A_3 R_1}{A_1 R_3}\right)\left[\frac{Exp(-\lambda_1\,0.5\Delta t)}{(\lambda_3 - \lambda_1)(\lambda_2 - \lambda_1)}\right.$$

$$\left. + \frac{Exp(-\lambda_2\,0.5\Delta t)}{(\lambda_3 - \lambda_2)(\lambda_1 - \lambda_2)} + \frac{Exp(-\lambda_3\,0.5\Delta t)}{(\lambda_2 - \lambda_3)(\lambda_1 - \lambda_3)}\right] + \lambda_2 c_2(t - \Delta t, x, y, z)\left(\frac{A_3 R_2}{A_2 R_3}\right)\left[\frac{Exp(-\lambda_2\,0.5\Delta t)}{(\lambda_3 - \lambda_2)}\right.$$

$$\left. + \frac{Exp(-\lambda_3\,0.5\Delta t)}{(\lambda_2 - \lambda_3)}\right] + c_3(t - \Delta t, x, y, z)\,Exp(-\lambda_3\,0.5\Delta t)$$

$$c_4(t - 0.5\Delta t, x, y, z) = \lambda_1 \lambda_2 \lambda_3 c_1(t - \Delta t, x, y, z)\left(\frac{A_4 R_1}{A_1 R_4}\right)\left[\frac{Exp(-\lambda_1\,0.5\Delta t)}{(\lambda_4 - \lambda_1)(\lambda_3 - \lambda_1)(\lambda_2 - \lambda_1)}\right.$$

$$+ \frac{Exp(-\lambda_2\,0.5\Delta t)}{(\lambda_4 - \lambda_2)(\lambda_3 - \lambda_2)(\lambda_1 - \lambda_2)} + \frac{Exp(-\lambda_3\,0.5\Delta t)}{(\lambda_4 - \lambda_3)(\lambda_2 - \lambda_3)(\lambda_1 - \lambda_3)}$$

$$\left. + \frac{Exp(-\lambda_4\,0.5\Delta t)}{(\lambda_3 - \lambda_4)(\lambda_2 - \lambda_4)(\lambda_1 - \lambda_4)}\right] + \lambda_2 \lambda_3 c_2(t - \Delta t, x, y, z)\left(\frac{A_4 R_2}{A_2 R_4}\right)\left[\frac{Exp(-\lambda_2\,0.5\Delta t)}{(\lambda_4 - \lambda_2)(\lambda_3 - \lambda_2)}\right.$$

$$\left. + \frac{Exp(-\lambda_3\,0.5\Delta t)}{(\lambda_4 - \lambda_3)(\lambda_2 - \lambda_3)} + \frac{Exp(-\lambda_4\,0.5\Delta t)}{(\lambda_3 - \lambda_4)(\lambda_2 - \lambda_4)}\right] + \lambda_3 c_3(t - \Delta t, x, y, z)\left(\frac{A_4 R_3}{A_3 R_4}\right)\left[\frac{Exp(-\lambda_3\,0.5\Delta t)}{(\lambda_4 - \lambda_3)}\right.$$

$$\left. + \frac{Exp(-\lambda_4\,0.5\Delta t)}{(\lambda_3 - \lambda_4)}\right] + c_4(t - \Delta t, x, y, z)\,Exp(-\lambda_4\,0.5\Delta t)$$

$$c_5(t - 0.5\Delta t, x, y, z) = \lambda_1 \lambda_2 \lambda_3 \lambda_4 c_1(t - \Delta t, x, y, z)\left(\frac{A_5 R_1}{A_1 R_5}\right)\left[\frac{Exp(-\lambda_1\,0.5\Delta t)}{(\lambda_5 - \lambda_1)(\lambda_4 - \lambda_1)(\lambda_3 - \lambda_1)(\lambda_2 - \lambda_1)}\right.$$

$$+ \frac{Exp(-\lambda_2\,0.5\Delta t)}{(\lambda_5 - \lambda_2)(\lambda_4 - \lambda_2)(\lambda_3 - \lambda_2)(\lambda_1 - \lambda_2)} + \frac{Exp(-\lambda_3\,0.5\Delta t)}{(\lambda_5 - \lambda_3)(\lambda_4 - \lambda_3)(\lambda_2 - \lambda_3)(\lambda_1 - \lambda_3)}$$

$$\left. + \frac{Exp(-\lambda_4\,0.5\Delta t)}{(\lambda_5 - \lambda_4)(\lambda_3 - \lambda_4)(\lambda_2 - \lambda_4)(\lambda_1 - \lambda_4)} + \frac{Exp(-\lambda_5\,0.5\Delta t)}{(\lambda_4 - \lambda_5)(\lambda_3 - \lambda_5)(\lambda_2 - \lambda_5)(\lambda_1 - \lambda_5)}\right]$$

$$+ \lambda_2 \lambda_3 \lambda_4 c_2(t - \Delta t, x, y, z)\left(\frac{A_5 R_2}{A_2 R_5}\right)\left[\frac{Exp(-\lambda_2\,0.5\Delta t)}{(\lambda_5 - \lambda_2)(\lambda_4 - \lambda_2)(\lambda_3 - \lambda_2)}\right.$$

$$+ \frac{Exp(-\lambda_3\,0.5\Delta t)}{(\lambda_5 - \lambda_3)(\lambda_4 - \lambda_3)(\lambda_2 - \lambda_3)} + \frac{Exp(-\lambda_4\,0.5\Delta t)}{(\lambda_5 - \lambda_4)(\lambda_3 - \lambda_4)(\lambda_2 - \lambda_4)}$$

$$\left. + \frac{Exp(-\lambda_5\,0.5\Delta t)}{(\lambda_4 - \lambda_5)(\lambda_3 - \lambda_5)(\lambda_2 - \lambda_5)}\right] + \lambda_3 \lambda_4 c_3(t - \Delta t, x, y, z)\left(\frac{A_5 R_3}{A_3 R_5}\right)\left[\frac{Exp(-\lambda_3\,0.5\Delta t)}{(\lambda_5 - \lambda_3)(\lambda_4 - \lambda_3)}\right.$$

$$\left. + \frac{Exp(-\lambda_4\,0.5\Delta t)}{(\lambda_5 - \lambda_4)(\lambda_3 - \lambda_4)} + \frac{Exp(-\lambda_5\,0.5\Delta t)}{(\lambda_4 - \lambda_5)(\lambda_3 - \lambda_5)}\right] + \lambda_4 c_4(t - \Delta t, x, y, z)\left(\frac{A_5 R_4}{A_4 R_5}\right)\left[\frac{Exp(-\lambda_4\,0.5\Delta t)}{(\lambda_5 - \lambda_4)}\right.$$

$$\left. + \frac{Exp(\lambda_5\,0.5\Delta t)}{(\lambda_4 - \lambda_5)}\right] + c_5(t - \Delta t, x, y, z)\,Exp(-\lambda_5\,0.5\Delta t)$$

(A1)

In the above equations, A is the atomic weight of the radionuclide, R is the retardation factor, c is the concentration of radionuclide, and the subscripts 1, 2, 3, 4, 5 designate the order of progeny in the decay chain. *Retardation factor* refers to the ratio of the migration velocity of water in the geological medium to that of radionuclide being carried. It is always larger than unity since the sorption of radionuclide by solid particles in the medium impedes the migration of radionuclide. The computer code for this process is implemented in the "decay" subroutine program.

Boundary Condition

Since this model deals with dispersion as the primary nature of transport, the radionuclide concentration at the boundary can be calculated by assuming the ratio of concentrations at the boundary and at the previous nodal point is a fixed fraction of the same ratio measured at the previous node. Based on the above assumption, the concentration of radionuclide at the boundary nodal point can be calculated from the concentration at the previous nodal point by:

$$c(t,E,x_1,x_2) = c(t,E-1,x_1,x_2) \cdot \eta \left\{ \frac{c(t,E-1,x_1,x_2)}{c(t,E-2,x_1,x_2)} \right\}$$

(A2)

in which, η is the dispersion tail coefficient, which is the fraction of the ratio of concentrations described above, E is the nodal point at the boundary, E-1 and E-2 are respectively the first and second nodal points immediately next to the boundary node, and x_1 and x_2 are the nodal points with respect to the other two axes.

Theoretically, the dispersion tail coefficient should vary with time, location of the diffusion plume tail, and characteristics of the diffusion plume. However, if the point is selected far enough from the diffusion source and the prime nature of the transport is limited to the dispersion, then the coefficient can be narrowed down to a very small range. An observation of more than 40 collected dispersion plume tail data indicates that these values fluctuate between 0.95 and 0.98. Therefore, a conservative fixed value of 0.98 is selected for this simulation model.

Appendix B. Bateman Equations

The Bateman equation (Bateman, 1910; Evans, 1967, P. 490) is used for the decay/ingrowth analysis. The number of atom at t target year takes the form:

$$N_1 = N_{01} Exp(-\lambda_1 t)$$

$$N_2 = \lambda_1 N_{01} \left[\frac{Exp(-\lambda_1 t)}{(\lambda_2 - \lambda_1)} + \frac{Exp(-\lambda_2 t)}{(\lambda_1 - \lambda_2)} \right]$$

$$N_3 = \lambda_1 \lambda_2 N_{01} \left[\frac{Exp(-\lambda_1 t)}{(\lambda_3 - \lambda_1)(\lambda_2 - \lambda_1)} + \frac{Exp(-\lambda_2 t)}{(\lambda_3 - \lambda_2)(\lambda_1 - \lambda_2)} + \frac{Exp(-\lambda_3 t)}{(\lambda_2 - \lambda_3)(\lambda_1 - \lambda_3)} \right]$$

$$N_4 = \lambda_1 \lambda_2 \lambda_3 N_{01} \left[\frac{Exp(-\lambda_1 t)}{(\lambda_4 - \lambda_1)(\lambda_3 - \lambda_1)(\lambda_2 - \lambda_1)} + \frac{Exp(-\lambda_2 t)}{(\lambda_4 - \lambda_2)(\lambda_3 - \lambda_2)(\lambda_1 - \lambda_2)} \right.$$
$$\left. + \frac{Exp(-\lambda_3 t)}{(\lambda_4 - \lambda_3)(\lambda_2 - \lambda_3)(\lambda_1 - \lambda_3)} + \frac{Exp(-\lambda_4 t)}{(\lambda_3 - \lambda_4)(\lambda_2 - \lambda_4)(\lambda_1 - \lambda_4)} \right]$$

$$N_5 = \lambda_1 \lambda_2 \lambda_3 \lambda_4 N_{01} \left[\frac{Exp(-\lambda_1 t)}{(\lambda_5 - \lambda_1)(\lambda_4 - \lambda_1)(\lambda_3 - \lambda_1)(\lambda_2 - \lambda_1)} \right.$$
$$+ \frac{Exp(-\lambda_2 t)}{(\lambda_5 - \lambda_2)(\lambda_4 - \lambda_2)(\lambda_3 - \lambda_2)(\lambda_1 - \lambda_2)} + \frac{Exp(-\lambda_3 t)}{(\lambda_5 - \lambda_3)(\lambda_4 - \lambda_3)(\lambda_2 - \lambda_3)(\lambda_1 - \lambda_3)}$$
$$\left. + \frac{Exp(-\lambda_4 t)}{(\lambda_5 - \lambda_4)(\lambda_3 - \lambda_4)(\lambda_2 - \lambda_4)(\lambda_1 - \lambda_4)} + \frac{Exp(-\lambda_5 t)}{(\lambda_4 - \lambda_5)(\lambda_3 - \lambda_5)(\lambda_2 - \lambda_5)(\lambda_1 - \lambda_5)} \right]$$

(B1)

where N is the number of atom, λ is the decay constant, t is the target year, subscripts 1, 2, 3, 4, and 5 represent the sequence of decay chain members, and subscript 0 denotes the initial value.

Acknowledgments

References

Anderson, M.P., and W.W. Woessner. 1992. *Applied Groundwater Modeling, Simulation of Flow and Advective Transport*. Academic Press, Inc., New York, NY.

Bateman, H. 1910. The solution of a system of differential equations occurring in the theory of radio-active transformations, *Proceedings of the Cambridge Philosophical Society* 15:423–427.

Bear, J., 1979. *Hydraulics of Groundwater*. McGraw-Hill, New York, NY.

Bird, R.B., W.E. Stewart, and E.N. Lightfoot. 1960. *Transport Phenomena*. John Wiley & Sons, Inc., New York, NY.

Burnett, R.D., and E.O. Frind. 1987. Simulation of contaminant transport in three dimensions, two dimensionality effects. *Water Resources Research* 23:695–705.

Chang, Z.S., J.D. Vervoort, W.C. McClelland, and C. Knaack. 2006. U-Pb dating of zircon by LA-ICP-MS. *Geochemistry Geophysics Geosystems*. 7: Art. No. Q05009. http://www.agu.org/journals/gc/

Compston, W., D.O. Froude, T.R. Ireland, P.D. Kinny, I.S. Williams, I.R. Williams, and J.S. Myers. 1985. The age of (a tiny part of) the Australian continent. *Nature* 17:559–560.

Crank, J. 1975. *The Mathematics of Diffusion*, 2nd ed. Oxford University Press, London, UK.

Duguid, J.O., and M. Reeves. 1976. Material transport through porous media—a finite-element Galerkin model. Environmental Science Division publication 733, Oak Ridge National Laboratory, ORNL-4298.

Durrance, E.M. 1986. *Radioactivity in Geology*. Ellis Horwood Limited, New York, NY.

Evans, R. D. 1967. *The Atomic Nucleus*. McGraw-Hill Book Company, New York, NY.

Getty, S.R., and D.J. DePaolo. 1995. Quaternary geochronology using the U-Th-Pb method. *Geochimica et Cosmochimica Acta* 59:3267–3272.

Hille, P. 1979. An open system model for uranium dating. *Earth and Planetary Science Letters* 42:138–142.

Hillel, D. 1980. *Fundamentals of Soil Physics*. Academic Press, New York, NY.

Ho, C.Y., Y.S. Touloukian, W.R. Judd, and R.F. Roy. 1989. *Physical Properties of Rocks and Minerals*—CINDAS Data Series on Material Properties, Vol. II-2. Hemisphere Publishing Corporation, New York, NY.

Hung, C.Y. 1983. A model to simulate infiltration of rainwater through the cover of a radioactive waste trench under saturated and unsaturated conditions. In Mercer, J.W., P.S.C. Rao, and I.W. Marine (editors), *Role of the Unsaturated Zone in Radioactive and Hazardous Waste Disposal*, pp. 27–48. Ann Arbor Science, Ann Arbor, MI.

Hung, C.Y. 1986. An optimum groundwater transport model for application to the assessment of health effects due to land disposal of radioactive waste. *Nuclear and Chemical Waste Management* 6:41–50.

Hung, C.Y. 2000. User's guide for PRESTO-EPA-CPG/POP operation system—a multimedia risk assessment model, Version 4.2. EPA report, Office of Radiation and Indoor Air, EPA 402-R-00-007. http://www.epa.gov/radiation/docs/assessment/402-r-00-007.pdf

Hung, C.Y. 2004. Isotopic geochronology by means of a dynamic simulation model—Part I. Uranium series method. Transactions, Geophysical Union 85: no. 47, pp. F1925. Presented at AGU Fall Meeting, San Francisco, December, 13–17.

Hung, C.Y. 2005. Dynamic model for calculating infiltration of rainwater through an unsaturated zone, and its application to Environmental Protection Agency's PRESTO model. *Practice Periodical of Hazardous, Toxic, and Radioactive Waste Management*, American Society of Civil Engineers 9:86–96.

Huyakorn, P.S., E.P. Springer, V. Guvanasen, and T.D. Wadsorth. 1986. A three-dimensional finite element model for simulating water flow in variably saturated porous media. *Water Resources Research* 22:790–1808.

Hydrogeologic, Inc. 1995. VAM3DF: Variably saturated analysis model in three-dimensions for the data fusion system, Documentation and User's Guide. Hydrogeologic, Inc., Virginia. http://www.hgl.com.

Hydrogeologic, Inc. 2001. MODFLOW-SURFACT software documentation, Version 2.2, Documentation and User's Guide. Hydrogeologic, Inc., Virginia, http://www.hgl.com.

Leake, S.A., and M.R. Lilly. 1997. Documentation of a computer program FHB1 for assignment of transient specified-flow and specified-head boundaries in applications of the modular finite-difference groundwater flow model. USGS Open-File Report 97–571.

McDonald, M.D., and A.W. Harbaugh. 1988. A modular three-dimensional finite-difference flow model (MODFLOW). *Techniques in Water Resources Investigations of the US Geological Survey, Book 6*.

Mundil, R., K.R. Ludwig, I. Metcalfe, and P.R. Renne. 2004. Age and timing of the permian mass extinctions—U/Pb dating of closed-system zircons. *Science* 305:1760–1763.

Neymark, L.A., Y.V. Amelin, and J.B. Paces. 2000. ^{206}Pb-^{230}Th-^{234}U-^{238}U and ^{207}Pb-^{235}U geochronology of Quaternary opal, Yucca Mountain, Nevada. *Geochimica et Cosmochimica Acta* 64:2913–2928.

Nier, A.O., R.W. Thompson, and B.F. Murphey, 1941. The isotopic constitution of lead and the measurement of geologic time, III. *Physical Review* 60:112–116.

Pike, A.W.G., R.E.M. Hedges, J.B. Paces, and P. van Calsteren. 2002. U-series dating of bone using the diffusion-adsorption model. *Geochimica et Cosmochimica Acta* 66:4273–4286.

Pinder, G.F., and W.G. Gray. 1977. *Finite Element Simulation in Surface and Subsurface Hydrology*. Academic Press, Inc., New York, NY.

Sandia National Laboratory (SNL). 1996. Performance evaluation of the technical capabilities of DOE sites for disposal of mixed low-level waste. DOE report, DOE/ID-10521, U.S. Department of Energy.

Scheidegger, A.E. 1961. General theory of dispersion in porous media. *Journal of Geophysical Research* 66:3273–3278.

Shleien, B., L.A., Slaback, and B.K. Birky. 1998. *Handbook of Health Physics and Radiological Health*. Williams & Wilkins, Philadelphia, PA.

Szabo, B.J., and J.N. Rosholt. 1969. Uranium-series dating of Pleistocene molluscan shells from southern California—an open system model. *Journal of Geophysical Research* 74:3253–3260.

Tera, F., and G.J. Wasserburg. 1972. U-Th-Pb systematic in three Apollo 14 basalts and the problem of initial Pb in lunar rocks. *Earth and Planetary Science Letters* 14:281–304.

Tera, F. 2003. A lead isotope method for the accurate dating of disturbed geologic systems—numerical demonstrations, some applications and implications. *Geochimica et Cosmochimica Acta* 67:3687–3716.

Thibodeaux, L.J. 1979. *Chemodynamics—Environmental Movement of Chemicals in Air, Water, and Soil.* John Wiley and Sons, Inc., New York, NY.

U.S. Army Waterways Experiment Station. 2002. Documentation of groundwater modeling system (GMS), Documentation and user's guide, Version 4.0. US Army Waterways Experiment Station, Vicksburg, MS.

U.S. Department of Energy (USDOE). 1992. Baseline assessment for the chemical plant area of the Weldon Spring site. DOE report, DOE/OR/21548-091, U.S. Department of Energy, Oak Ridge Field Office, Oak Ridge, TN.

U.S. Department of Health, Education, and Welfare. 1970. *Radiological Health Handbook*. U.S. Government Printing Office, Rockville, MD.

U.S. Environmental Protection Agency (USEPA) 1999a. Understanding variation in partition coefficient, K_d, values, volume II: review of geochemistry and available K_d values for cadmium, cesium, chromium, lead, plutonium, radon, strontium, thorium, tritium (^3H), and uranium. EPA report, EPA 402-R-99-004B.

U.S. Environmental Protection Agency (USEPA). 1999b. Draft background information document for 40 CFR Part 193—propose rule for land disposal of low-activity mixed waste. Unpublished EPA report.

Van Calsteren, P., and L. Thomas. 2006. Uranium-series dating applications in natural environmental science. *Earth-Science Reviews* 75:155–175.

Wetherill, G.W. 1956. Discordant uranium-lead ages I. *Transactions of the American Geophysical Union* 37:320–326.

Yeh, G.T., H.J. Lin, D.R. Richards, C.A. Talbot, J.R. Cheng, H.P. Cheng, and N.L. Jones. 2002. FEMWATER—A three dimensional finite element computer model for simulating density-dependent flow and transport in variably saturated media—documentation of groundwater modeling system (GMS), Version 4.0. U.S. Army Waterways Experiment Station, Vicksburg, MS.

Erratum

In "Origins of Apoptosis," page 207 of the Winter 2008 *CRSQ*, the statement should be: "Cells (such as melanin cells) that are not prone to UV damage produce very small amounts of apoptosis-inhibiting Bcl-2 protein."